Efficient generation of propagation-invariant spatially stationary partially coherent fields

Shaurya Aarav, Abhinandan Bhattacharjee, Harshawardhan Wanare, and Anand K. Jha*
Department of Physics, Indian Institute of Technology, Kanpur 208016, India

(Received 18 July 2017; published 8 September 2017)

We propose and demonstrate a method for generating propagation-invariant spatially stationary fields in a controllable manner. Our method relies on producing incoherent mixtures of plane waves using planar primary sources that are spatially completely uncorrelated. The strengths of the individual plane waves in the mixture determine the exact functional form of the generated coherence function. We use light-emitting diodes as the primary incoherent sources and experimentally demonstrate the effectiveness of our method by generating several spatially stationary fields, including a type that we refer to as the regionwise spatially stationary field. We also experimentally demonstrate the propagation invariance of these fields, which is an extremely interesting and useful property of such fields. Our work should have important implications for applications that exploit the spatial coherence properties either in a transverse plane or in a propagation-invariant manner, such as correlation holography, wide-field optical coherence tomography, and imaging through turbulence.

DOI: 10.1103/PhysRevA.96.033815

I. INTRODUCTION

Fields having partial spatial coherence have been extensively studied in the past few decades [1–3] and have found a wide range of applications including wide-field optical coherence tomography (OCT) [4], imaging through turbulence [5], optical communication [6,7], particle trapping [8,9], atomic optics [10], laser scanning [11], plasma instability suppression [12], photographic noise reduction [13], optical scattering [14], and second-harmonic generation [15]. A spatially partially coherent field can be divided into two categories: spatially stationary and spatially nonstationary. In analogy with the temporally stationary fields, when the intensity of a field is independent of the spatial position and when the two-point spatial correlation function depends on the spatial positions only through their difference, the field is called spatially stationary, at least in the wide sense [16–25]. A spatially stationary field has the unique property that its two-point correlation function is propagation invariant [19,25]. Propagation-invariant spatially stationary fields have several unique applications such as three-dimensional (3D) coherence holography [23] and photon correlation holography [24]. If the field is not spatially stationary, it is categorized as spatially nonstationary.

There are several different ways of producing spatially partially coherent fields. While one of the earliest experiments used a laser and an acousto-optical cell [25], later experiments utilized a laser and a rotating ground glass plate (RGGP) in order to produce fields with desired partial spatial coherence [16,23,26–32]. More modern methods involve using a laser and either a spatial light modulator (SLM) [33–36] or an RGGP in combination with an SLM to achieve the purpose [24,37,38]. As far as propagation-invariant spatially stationary partially coherent fields are concerned, we are aware of only two experimental studies. In the first experiment the field was generated using a laser and an acousto-optic cell [25] and in the second experiment the generation was done using a laser and an RGGP [19]. Nevertheless, both these techniques have demonstrated generation of only those cross-spectral density functions that can be represented as Fourier transforms of circularly symmetric functions.

Thus, all the existing experimental techniques for producing spatially stationary partially coherent fields and most techniques for producing spatially nonstationary partially coherent fields use a laser as the primary source, which, to begin with, is spatially a completely correlated source. One then tries to make the field emanating from such a source spatially partially coherent by introducing randomness in the field path by using either an acousto-optic cell [25], or an RGGP [16,23,26–32] or an SLM [24,33–38]. On the other hand, in this article we propose a technique that uses a primary source that is spatially completely uncorrelated and we demonstrate generation of very-high-quality propagation-invariant spatially stationary fields, without having to introduce any additional randomness. Furthermore, we show that our technique can produce any propagation-invariant spatially stationary cross-spectral density function and not just the ones that are Fourier transforms of circularly symmetric functions [19,25].

II. THEORY: PROPAGATION-INVARIANT SPATIALLY STATIONARY PARTIALLY COHERENT FIELDS

Let us consider the situation shown in Fig. 1. A planar, monochromatic, spatially completely incoherent primary source is kept at the back focal plane $z = -f$ of a lens kept at $z = 0$. The planar primary source along with the lens constitutes our source of spatially partially coherent fields. We represent the field radiating out from spatial location $\boldsymbol{\rho}'$ at z by $V_s(\boldsymbol{\rho}',z)$. Since our primary source is spatially completely incoherent, the fields $V_s(\boldsymbol{\rho}_1',-f)$ and $V_s(\boldsymbol{\rho}_2',-f)$ radiating out from $\boldsymbol{\rho}_1'$ and $\boldsymbol{\rho}_2'$, respectively, at $z=-f$ are completely uncorrelated, that is,

$$\langle V_s^*(\boldsymbol{\rho}_1',-f)V_s(\boldsymbol{\rho}_2',-f)\rangle_e = I_s(\boldsymbol{\rho}_1',-f)\delta(\boldsymbol{\rho}_1'-\boldsymbol{\rho}_2'). \quad (1)$$

Here $I_s(\boldsymbol{\rho}_1',-f)$ is the intensity of the primary source at $z=-f$. We note that no realistic primary source can truly have a position correlation given by Eq. (1), which requires that the spatial coherence length be zero. The smallest spatial coherence length that can be associated with a primary source is of the order of the wavelength λ of the source and

*akjha9@gmail.com

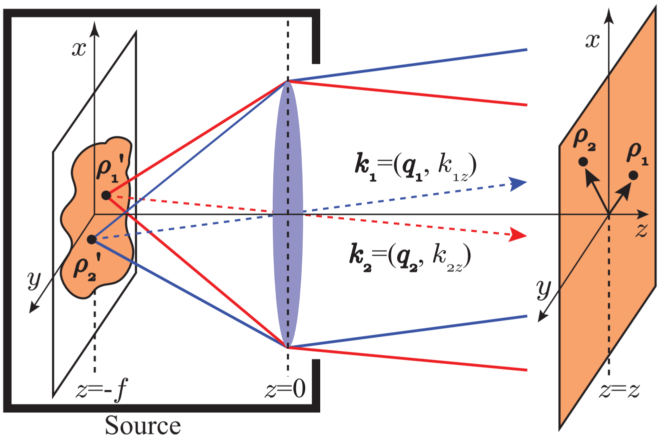

FIG. 1. Schematic illustration of how a propagation-invariant spatially stationary field can be generated using a spatially completely uncorrelated primary source.

only a blackbody emitter can be idealized as such a source [39]. Nevertheless, for a millimeter-size source at optical wavelengths, the position correlations of the order of λ can very well be approximated by Eq. (1). In our experiments, we use light-emitting diodes (LEDs) as our primary incoherent sources, which are considered spatially completely incoherent in the sense that their position correlations are approximated by the form given in Eq. (1) [40,41].

Thus, for our primary source whose position correlation is represented by Eq. (1), every point on the source is radiating out as an independent point source and since each of these points is kept at the back focal plane of a converging lens, the field $V_s(\boldsymbol{\rho}_1',-f)$ radiating out from $\boldsymbol{\rho}_1'$ gets transformed into a plane wave with amplitude $a(\boldsymbol{q_1})$ by the lens, where $\boldsymbol{q_1}$ represents the transverse wave vector associated with the plane wave [42,43]. Here we are assuming that the aperture size of the lens is infinite. This turns out to be a very good approximation for our purposes in this section and the next; the effects due to a finite-aperture-size lens are discussed and demonstrated in Sec. IV. The lens, therefore, transforms the noncorrelation of the planar source in the position basis to noncorrelation in the transverse-wave-vector basis. The correlations between different transverse wave vectors are quantified using the angular correlation function $\mathcal{A}(\boldsymbol{q}_1,\boldsymbol{q}_2)$, which is defined as $\mathcal{A}(\boldsymbol{q}_1,\boldsymbol{q}_2)\equiv\langle a^*(\boldsymbol{q}_1)a(\boldsymbol{q}_2)\rangle_e$, where $\langle\cdots\rangle_e$ represents the ensemble average. The angular correlation function of our partially coherent source is the angular correlation function $\mathcal{A}(\boldsymbol{q}_1,\boldsymbol{q}_2)$ at the exit face of the lens, that is, at $z=0$, and is thus given by

$$\mathcal{A}(\boldsymbol{q}_1,\boldsymbol{q}_2)\equiv\langle a^*(\boldsymbol{q}_1)a(\boldsymbol{q}_2)\rangle_e=I_s(\boldsymbol{q}_1)\delta(\boldsymbol{q}_1-\boldsymbol{q}_2). \quad (2)$$

Here $I_s(\boldsymbol{q}_1)$ is the spectral density of the field; it has the same functional form as that of the source intensity. As we show below, this form of the angular correlation function is *the* requirement for the partially coherent field coming out of a source to be spatially stationary and propagation invariant.

We next derive the cross-spectral density function at $z=z$ produced by our source. As worked out in Sec. 5.6 of Ref. [1], if the plane-wave amplitude at $z=0$ is $a(\boldsymbol{q}_1)$, then the field $V(\boldsymbol{\rho}_1,z)$ at $z=z$ within the paraxial approximation is given by

$$V(\boldsymbol{\rho}_1,z)=e^{ik_0z}\iint_{-\infty}^{\infty}a(\boldsymbol{q}_1)e^{i\boldsymbol{q}_1\cdot\boldsymbol{\rho}_1}e^{-i(q_1^2z/2k_0)}d\boldsymbol{q}_1. \quad (3)$$

Here we have used the fact that $\boldsymbol{r_1}\equiv(\boldsymbol{\rho}_1,z)$, $\boldsymbol{k}_1\equiv(\boldsymbol{q}_1,k_{1z})$, and $k_{1z}\approx k_1-q_1^2/2k_1$, with $q_1=|\boldsymbol{q}_1|$ and $k_1=|\boldsymbol{k}_1|=k_0=\omega_0/c$, where ω_0 is the frequency of the field. The cross-spectral density function $W(\boldsymbol{\rho}_1,\boldsymbol{\rho}_2,z)\equiv\langle V^*(\boldsymbol{\rho}_1,z)V(\boldsymbol{\rho}_2,z)\rangle_e$ at $z=z$ is therefore

$$W(\boldsymbol{\rho}_1,\boldsymbol{\rho}_2,z)=\iint_{-\infty}^{\infty}\mathcal{A}(\boldsymbol{q}_1,\boldsymbol{q}_2)\times e^{-i\boldsymbol{q}_1\cdot\boldsymbol{\rho}_1+i\boldsymbol{q}_2\cdot\boldsymbol{\rho}_2}e^{-i[(q_1^2-q_2^2)z/2k_0]}d\boldsymbol{q}_1d\boldsymbol{q}_2. \quad (4)$$

Equation (4) governs how spatial correlations of the field, as represented by the cross-spectral density function, change upon propagation in the region $z>0$ after the lens. Substituting the form of the angular correlation function from Eq. (2) into Eq. (4), we obtain

$$W(\boldsymbol{\rho}_1,\boldsymbol{\rho}_2,z)=W(\boldsymbol{\Delta}\rho,z)=\int_{-\infty}^{\infty}I_s(\boldsymbol{q})e^{-i\boldsymbol{q}\cdot\boldsymbol{\Delta}\boldsymbol{\rho}}d\boldsymbol{q}, \quad (5)$$

where $\boldsymbol{\Delta}\rho=\boldsymbol{\rho}_1-\boldsymbol{\rho}_2$. The intensity $I(\boldsymbol{\rho},z)$ corresponding to the above cross-spectral density function is

$$I(\boldsymbol{\rho},z)=W(\boldsymbol{\rho},\boldsymbol{\rho},z)=\int_{-\infty}^{\infty}I_s(\boldsymbol{q})d\boldsymbol{q}=K, \quad (6)$$

where K is a constant. We find that the cross-spectral density function $W(\boldsymbol{\Delta}\rho,z)$ in Eq. (5) is in the coherent-mode representation, with the plane waves being the coherent modes. In other words, our source produces a field that is an incoherent mixture of plane-wave modes. As a result, the generated field has the following properties. (i) The field is propagation invariant. This is because the cross-spectral density function as well as the intensity is independent of z. (ii) The field is spatially stationary at a given z, at least in the wide sense. This can be verified by noting that the intensity $I(\boldsymbol{\rho},z)$ does not depend on $\boldsymbol{\rho}$ and the cross-spectral density function depends on $\Delta\boldsymbol{\rho}$ only. (iii) The cross-spectral density function $W(\boldsymbol{\Delta}\rho,z)$ of the field is the Fourier transform of its spectral density $I_s(\boldsymbol{q})$. This is the spatial analog of the Wiener-Khintchine theorem for temporally stationary fields (see Sec. 2.4 of [1]). Moreover, since the spectral density has the same functional form as the intensity of the primary source, the cross-spectral density function of the field is the Fourier transform of the intensity profile of the primary source. We note that in our technique there is no restriction on the form of the intensity function $I_s(\boldsymbol{q}_1)$ that the primary incoherent source can have. The primary source can be continuous or having a finite size or even in the form of a collection of points. As a result, using our technique, one can produce any custom-designed, spatially stationary, propagation-invariant partially coherent field and not just the ones that are Fourier transforms of circularly symmetric functions [19,25].

III. EXPERIMENTAL DEMONSTRATIONS

Figure 2(a) shows the schematic of our experimental setup. Our primary source is a commercially available 9-W planar LED bulb. We use an interference filter centered at 632.8 nm

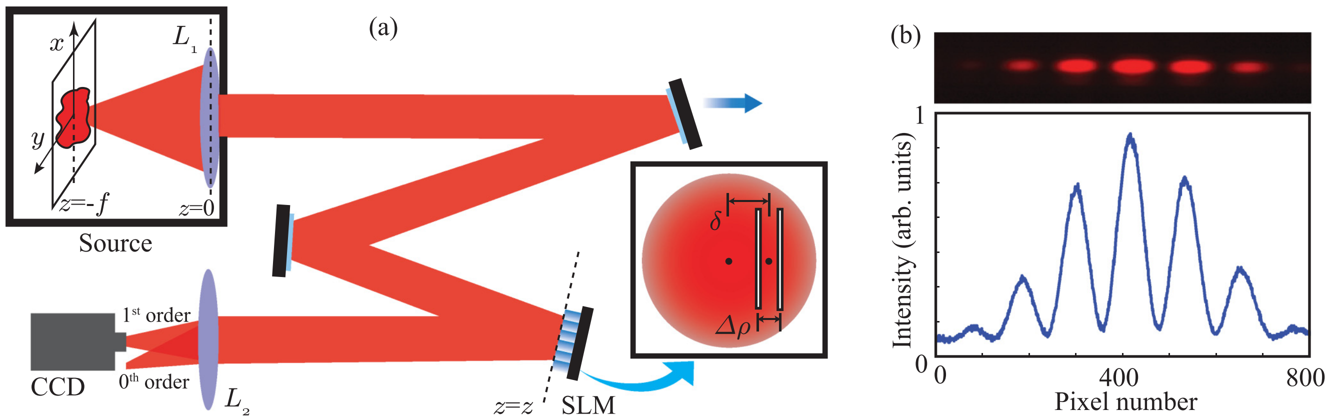

FIG. 2. (a) Schematic diagram of the experimental setup. A planar, spatially incoherent primary source is placed at the back focal plane of lens L_1. The cross-spectral density of the field produced by the source is measured using the spatial light modulator. The propagation length z is the distance between the lens L_1 and the SLM, and the CCD camera is placed at the focal plane of lens L_2. (b) Representative experimental interference pattern produced by the double-slit simulated on the SLM and the associated one-dimensional plot.

having a wavelength bandwidth of 10 nm. The LED bulb consists of nine separate LEDs arranged in a 3×3 grid. We take the individual LEDs to be spatially completely incoherent [40,41] in the sense that their spatial-correlation function can be approximated by Eq. (1). The individual LEDs are of dimensions 0.8×0.8 mm^2 and the separation between two nearest LEDs is 1.9 mm. We let the field produced by our source at $z = 0$ propagate to $z = z$ and then measure the cross-spectral density function using a Young double-slit pattern simulated on an SLM kept at $z = z$ [44–46], with the separation between the slits being $\boldsymbol{\Delta}\rho$. The distance between the center of the field and the center of the double slit is the offset parameter δ. We record the resulting interference fringe pattern by keeping a CCD camera at the focal plane of lens L_2 and then capturing only the first diffraction order due to the SLM. We note that since the two simulated slits are exactly the same and since the field is uniform in intensity, the magnitude $|W(\boldsymbol{\Delta}\rho,z)|$ of the cross-spectral density function is the visibility of interference fringes. Therefore, by measuring the interference visibility as a function of the slit separation $\boldsymbol{\Delta}\rho$, we directly measure $|W(\boldsymbol{\Delta}\rho,z)|$ as a function of $\boldsymbol{\Delta}\rho$. We further note that any pattern simulated on an SLM is seen by only one polarization component of an incoming field [46] and it is only this component that contributes at the first diffraction order. The other polarization component, if present, simply ends up at the zeroth diffraction order. Since our measurements are made only at the first diffraction order, only one polarization component gets measured and therefore scalar theory of Sec.II should be sufficient to describe the present experiments.

A typical interference pattern observed using the CCD camera and the associated one-dimensional section of the intensity pattern are shown in Fig. 2(b). Figure 3(a) is the image of the central LED of our bulb. First of all, we make measurements with this being our primary source. The focal length f of lens L_1 is 75 cm. Figure 3(b) shows the plot of the intensity at $z = 147$ cm and Fig. 3(c) shows plots of $|W(\boldsymbol{\Delta}\rho,z)|$ at $z = 147$ cm as a function of $\boldsymbol{\Delta}\rho$ for several offset values δ. These results verify that the generated field is spatially stationary. Figure 3(d) shows plots of $|W(\boldsymbol{\Delta}\rho,z)|$ as a function of $\boldsymbol{\Delta}\rho$ for various propagation distances up to 3.9 m. There is little variation between the different plots. This proves that the cross-spectral density function of the generated field is propagation invariant at least up to a distance of 3.9 m. We note that the transverse coherence length of the field, which we define to be the value of $\boldsymbol{\Delta}\rho$ at which $|W(\boldsymbol{\Delta}\rho,z)|$ drops down to $1/e$, is about 0.5 mm and remains propagation invariant. This is in contrast to the field produced by a bare primary source of the same shape and size as that of the source in Fig. 3(a), in which case the transverse coherence length, following the conventional van Cittert–Zernike theorem, increases by about 5 times after propagating for 3.9 m.

Next we make measurements with our primary source containing two spatially separated LEDs. The image of the primary source is shown in Fig. 4(a). Figure 4(b) shows the plot of the intensity at $z = 65$ cm. Figure 4(c) shows plots of $|W(\boldsymbol{\Delta}\rho,z)|$ as a function of $\boldsymbol{\Delta}\rho$ for various values of the offset parameter δ at $z = 65$ cm and Fig. 4(d) shows plots of $|W(\boldsymbol{\Delta}\rho,z)|$ as a function of $\boldsymbol{\Delta}\rho$ at various z. These results again demonstrate spatial stationarity and propagation invariance. It is interesting to note that the cross-spectral density function in this case is in the form of a fringe pattern, which is nothing but the Fourier transform of our source shown in Fig. 4(a).

Using Eq. (5) and the image of our primary sources shown in Figs. 3(a) and 4(a), we also calculate the theoretical cross-spectral density functions and plot them along with the experimental results in Figs. 3 and 4. Our reported experimental results match very well with the theoretical predictions, demonstrating the accuracy and effectiveness with which a custom-designed, spatially stationary, propagation-invariant cross-spectral density function can be generated using our method. In order to produce a field with a given cross-spectral density function one simply needs to construct a primary source with an intensity distribution that is the inverse Fourier transform of the desired cross-spectral density function.

IV. EFFECTS DUE TO A FINITE-SIZE LENS

The theoretical modeling presented so far assumes that the lens that constitutes our partially coherent source has an infinite

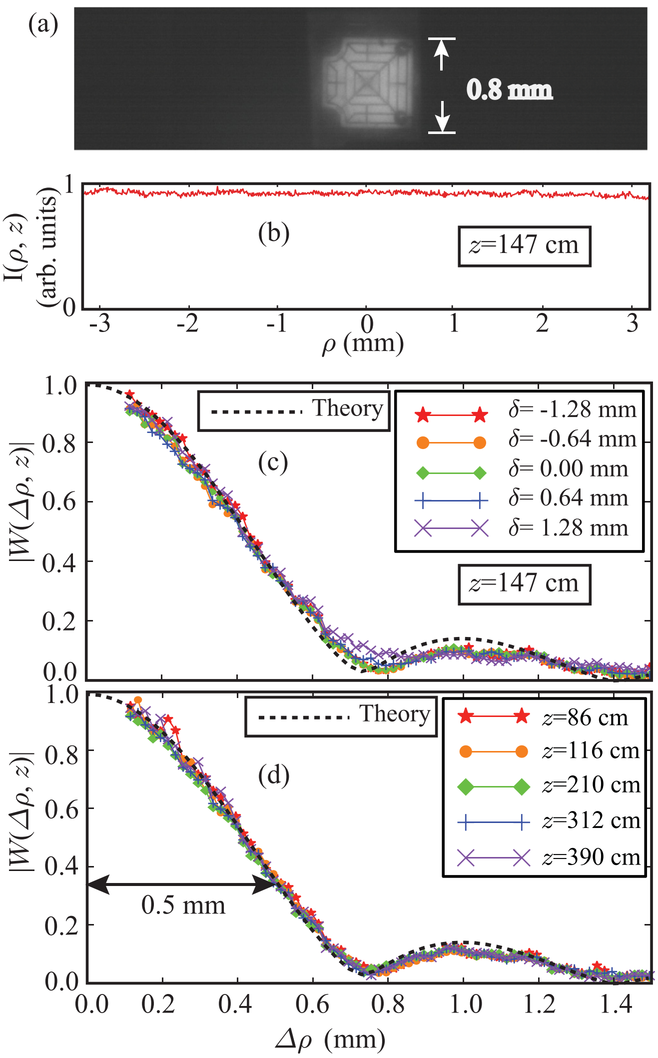

FIG. 3. (a) The CCD camera image of the LED. (b) Plot of intensity $I(\boldsymbol{\rho},z)$ as a function of $\boldsymbol{\rho}$ at $z = 147$ cm. (c) Plots of $|W(\boldsymbol{\Delta}\rho,z)|$ as a function of $\boldsymbol{\Delta}\rho$ at $z = 147$ cm for various values of the offset parameter δ. (d) Plot of $|W(\boldsymbol{\Delta}\rho,z)|$ as a function of $\boldsymbol{\Delta}\rho$ for various values of z. In (c) and (d) the black dashed curves represent the theoretical prediction based on Eq. (5).

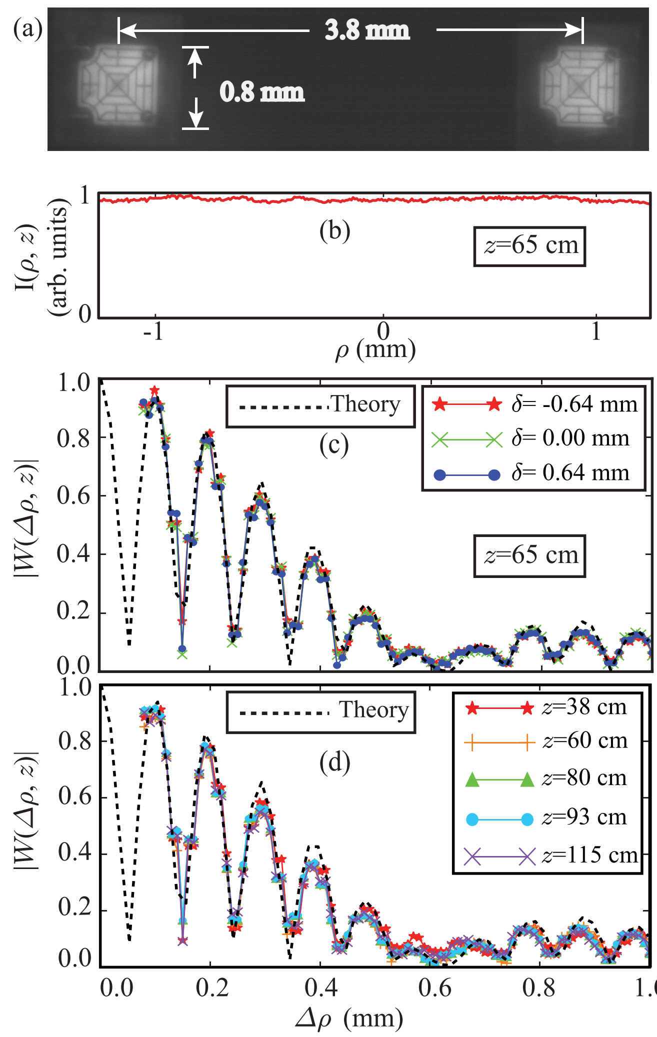

FIG. 4. (a) The CCD camera image of the LED. (b) Plot of intensity $I(\boldsymbol{\rho},z)$ as a function of $\boldsymbol{\rho}$ at $z = 65$ cm. (c) Plot of $|W(\boldsymbol{\Delta}\rho,z)|$ as a function of $\boldsymbol{\Delta}\rho$ at $z = 65$ cm for various values of the offset parameter δ. (d) Plot of $|W(\boldsymbol{\Delta}\rho,z)|$ as a function of $\boldsymbol{\Delta}\rho$ for various values of z. In (c) and (d) the black dashed curves represent the theoretical prediction based on Eq. (5).

aperture size. However, in a realistic experimental situation the aperture size of a lens is finite and in our case it is of the order of 1 in. As discussed in Ref. [19] and as illustrated in Fig. 5(a), the finite aperture size of the lens restricts the propagation invariance properties to a distance $z_{\max}$, given by $z_{\max} = Df/s$, where D is the aperture size of the lens, f is the focal length, and s is the size of the primary source. In order to experimentally demonstrate $z_{\max}$, we used the LED source shown in Fig. 3(a) with an $f = 30$ cm lens. Figures 5(b) and 5(c) show how the transverse coherence length changes as a function of z for two different values of the aperture size D. As the aperture-size becomes bigger, $z_{\max}$ gets larger. Nevertheless, even with realistic aperture sizes, one can easily achieve a $z_{\max}$ of up to tens of meters.

Although the finite aperture size of the lens may seem to only have the restricting effect on $z_{\max}$, it can in fact lead to restructuring of spatial correlations in a way that can have its own set of advantages. We now report such a restructuring effect when the primary source is in the form of two spatially separated LEDs, as shown in Fig. 4(a). As illustrated in Fig. 6(a), the propagation-invariant field generated due to such a primary source has two distinct regions over which spatial stationarity is observed. Region I receives plane-wave contributions from both the LEDs, while region II receives the contributions from a single LED only. This leads to the two regions having two distinct spatially stationary propagation-invariant cross-spectral density functions. We refer to such fields as regionwise spatially stationary fields. Figure 6(c) shows the plot of $|W(\boldsymbol{\Delta}\rho,z)|$ as a function of $\boldsymbol{\Delta}\rho$ for various values of the offset parameter δ in region II. These results demonstrate the spatial stationarity in region II. The spatial stationarity of region I is already shown in Fig. 4(c). Therefore, the finite aperture size of the lens offers an advantage in creating regionwise spatially stationary fields.

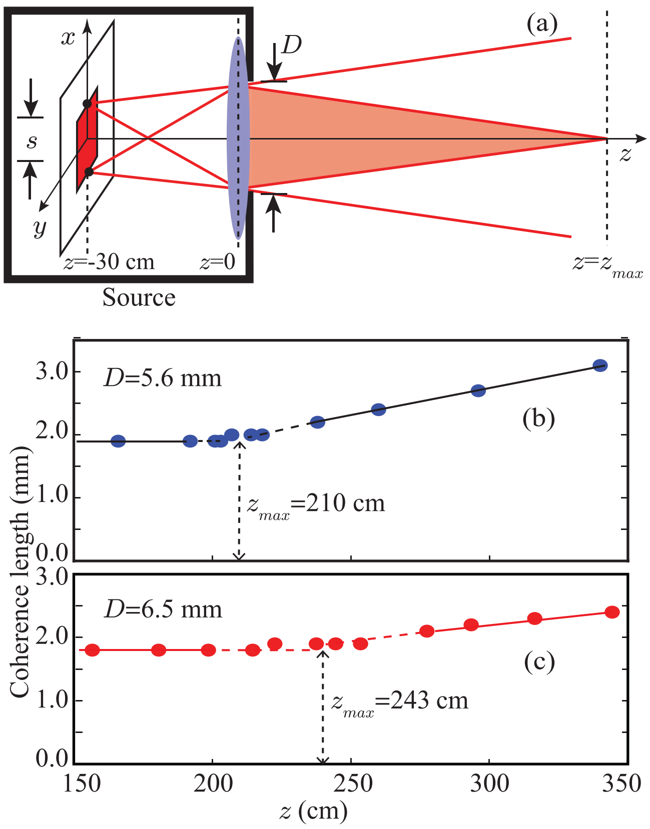

FIG. 5. (a) Diagram illustrating how the aperture size D of the lens and the spatial width s of the primary source fixes $z_{\max}$. Also shown are plots of the transverse coherence length as a function of z for (b) $D = 5.6$ mm and (c) $D = 6.5$ mm.

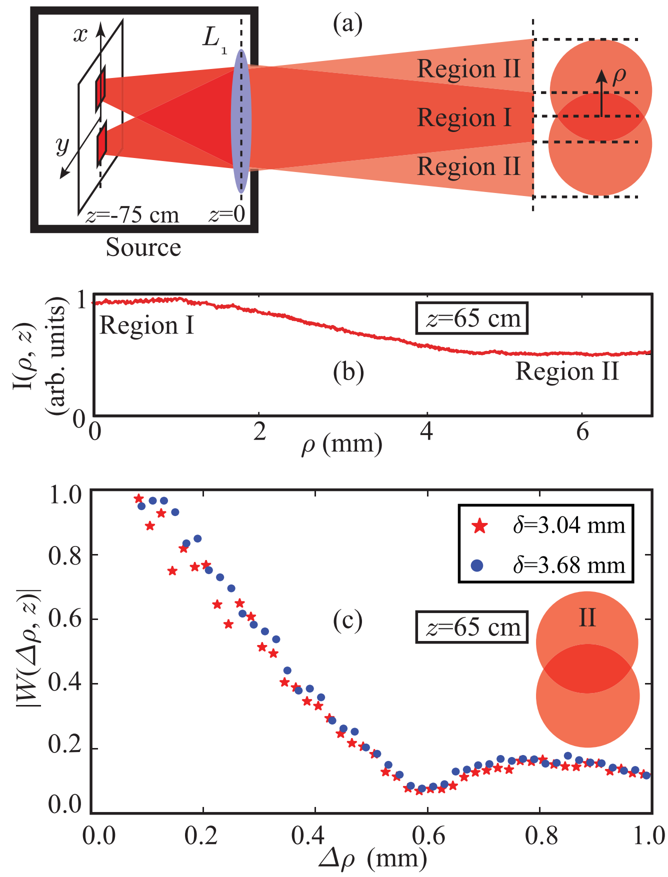

FIG. 6. (a) Diagram illustrating the generation of regionwise spatially stationary fields. (b) Plot of intensity $I(\boldsymbol{\rho},z)$ as a function of $\boldsymbol{\rho}$ at $z = 65$ cm. (c) Plot of $|W(\boldsymbol{\Delta}\rho,z)|$ as a function of $\boldsymbol{\Delta}\rho$ at $z = 65$ cm for various values of the offset parameter δ.

V. CONCLUSION

We have proposed and demonstrated a method for generating custom-designed, propagation-invariant, spatially stationary fields. Our method can be used for generating any spatially stationary cross-spectral density function as long as it has a coherent-mode representation in the plane-wave basis. Our experimental technique is based on using a spatially uncorrelated primary source and does not require introduction of any additional randomness, as is required by most other conventional methods. We have experimentally demonstrated the effectiveness of this technique by generating different spatially stationary fields, including a regionwise spatially stationary field. We have also demonstrated propagation invariance up to a few meters for several of these spatially stationary fields. The high efficiency and control inherent in our technique can have important practical implications for several applications. The propagation-invariant spatially stationary fields are already a necessity for applications such as correlation holography [23,24]. We believe that such fields can be an enabler for the 3D version of imaging through turbulence [5] and wide-field OCT [4]. Moreover, the regionwise spatially stationary fields could provide unique benefits when the feature sizes are spatially nonuniform.

ACKNOWLEDGMENTS

We acknowledge financial support through Initiation Grant No. IITK /PHY /20130008 from Indian Institute of Technology Kanpur, India and through a research grant from the Science and Engineering Research Board, Department of Science and Technology, Government of India, No. EMR/2015/001931.

[1] L. Mandel and E. Wolf, *Optical Coherence and Quantum Optics* (Cambridge University Press, New York, 1995).

[2] Y. Cai, Y. Chen, and F. Wang, J. Opt. Soc. Am. A **31**, 2083 (2014).

[3] M. W. Hyde IV, S. Basu, D. G. Voelz, and X. Xiao, J. Appl. Phys. **118**, 093102 (2015).

[4] B. Karamata, P. Lambelet, M. Laubscher, R. Salathé, and T. Lasser, Opt. Lett. **29**, 736 (2004).

[5] B. Redding, M. A. Choma, and H. Cao, Nat. Photon. **6**, 355 (2012).
[6] J. C. Ricklin and F. M. Davidson, J. Opt. Soc. Am. A **19**, 1794 (2002).
[7] Y. Gu and G. Gbur, J. Opt. Soc. Am. A **27**, 2621 (2010).
[8] C. Zhao, Y. Cai, X. Lu, and H. T. Eyyuboğlu, Opt. Express **17**, 1753 (2009).
[9] Y. Dong, F. Wang, C. Zhao, and Y. Cai, Phys. Rev. A **86**, 013840 (2012).
[10] G. R. M. Robb and W. J. Firth, Phys. Rev. Lett. **99**, 253601 (2007).
[11] D. Kermisch, J. Opt. Soc. Am. **65**, 887 (1975).
[12] Y. Kato, K. Mima, N. Miyanaga, S. Arinaga, Y. Kitagawa, M. Nakatsuka, and C. Yamanaka, Phys. Rev. Lett. **53**, 1057 (1984).
[13] A. Beléndez, L. Carretero, and A. Fimia, Opt. Commun. **98**, 236 (1993).
[14] T. van Dijk, D. G. Fischer, T. D. Visser, and E. Wolf, Phys. Rev. Lett. **104**, 173902 (2010).
[15] M. S. Zubairy and J. K. McIver, Phys. Rev. A **36**, 202 (1987).
[16] M. Takeda, W. Wang, Z. Duan, and Y. Miyamoto, Opt. Express **13**, 9629 (2005).
[17] M. Takeda, Opt. Lett. **38**, 3452 (2013).
[18] M. Takeda, W. Wang, D. N. Naik, and R. K. Singh, Opt. Rev. **21**, 849 (2014).
[19] J. Turunen, A. Vasara, and A. T. Friberg, J. Opt. Soc. Am. A **8**, 282 (1991).
[20] A. T. Friberg, A. Vasara, and J. Turunen, Phys. Rev. A **43**, 7079 (1991).
[21] M. W. Kowarz and G. S. Agarwal, J. Opt. Soc. Am. A **12**, 1324 (1995).
[22] F. Gori, G. Guattari, and C. Padovani, Opt. Commun. **64**, 311 (1987).
[23] D. N. Naik, T. Ezawa, Y. Miyamoto, and M. Takeda, Opt. Express **17**, 10633 (2009).
[24] D. N. Naik, R. K. Singh, T. Ezawa, Y. Miyamoto, and M. Takeda, Opt. Express **19**, 1408 (2011).
[25] Y. Ohtsuka, Y. Nozoe, and Y. Imai, Opt. Commun. **35**, 157 (1980).
[26] Y. Chen, F. Wang, L. Liu, C. Zhao, Y. Cai, and O. Korotkova, Phys. Rev. A **89**, 013801 (2014).
[27] Y. Chen, L. Liu, F. Wang, C. Zhao, and Y. Cai, Opt. Express **22**, 13975 (2014).
[28] F. Wang, C. Liang, Y. Yuan, and Y. Cai, Opt. Express **22**, 23456 (2014).
[29] A. S. Ostrovsky, G. Rodríguez-Zurita, C. Meneses-Fabián, M. Á. Olvera-Santamaría, and C. Rickenstorff-Parrao, Opt. Express **18**, 12864 (2010).
[30] F. Wang, X. Liu, Y. Yuan, and Y. Cai, Opt. Lett. **38**, 1814 (2013).
[31] F. Wang, Y. Cai, Y. Dong, and O. Korotkova, Appl. Phys. Lett. **100**, 051108 (2012).
[32] F. Wang and Y. Cai, Opt. Lett. **33**, 1795 (2008).
[33] S. Basu, M. W. Hyde, X. Xiao, D. G. Voelz, and O. Korotkova, Opt. Express **22**, 31691 (2014).
[34] A. S. Ostrovsky, G. Martínez-Niconoff, V. Arrizón, P. Martínez-Vara, M. A. Olvera-Santamaría, and C. Rickenstorff-Parrao, Opt. Express **17**, 5257 (2009).
[35] A. Ostrovsky, M. Olvera, C. Rickenstorff, G. Martínez-Niconoff, and V. Arrizón, Opt. Commun. **283**, 4490 (2010).
[36] T. Shirai and E. Wolf, J. Opt. Soc. Am. A **21**, 1907 (2004).
[37] C. Liang, F. Wang, X. Liu, Y. Cai, and O. Korotkova, Opt. Lett. **39**, 769 (2014).
[38] Y. Chen, F. Wang, C. Zhao, and Y. Cai, Opt. Express **22**, 5826 (2014).
[39] W. Carter and E. Wolf, J. Opt. Soc. Am. **67**, 785 (1977).
[40] M. Tziraki, R. Jones, P. French, M. Melloch, and D. Nolte, Appl. Phys. B **70**, 151 (2000).
[41] H. D. L. Pires, J. Woudenberg, and M. van Exter, Opt. Lett. **35**, 889 (2010).
[42] M. Born and E. Wolf, *Principles of Optics: Electromagnetic Theory of Propagation, Interference and Diffraction of Light* (Cambridge University Press, New York, 1999).
[43] J. W. Goodman, *Introduction to Fourier Optics* (Roberts, Englewood, 2005).
[44] N. Savage, Nat. Photon. **3**, 170 (2009).
[45] M. T. Gruneisen, W. A. Miller, R. C. Dymale, and A. M. Sweiti, Appl. Opt. **47**, A32 (2008).
[46] K. M. Johnson, D. J. McKnight, and I. Underwood, IEEE J. Quantum Electron. **29**, 699 (1993).